Geosci. Model Dev. Discuss., 5, 1949–1985, 2012
www.geosci-model-dev-discuss.net/5/1949/2012/
doi:10.5194/gmdd-5-1949-2012

Geoscientific Model Development Discussions

Tagged ozone mechanism for MOZART-4, CAM-chem, and other chemical transport models

L. K. Emmons[1], P. G. Hess[2], J.-F. Lamarque[1], and G. G. Pfister[1]

[1]Atmospheric Chemistry Division, National Center for Atmospheric Research, Boulder, CO, USA
[2]Department of Biological and Environmental Engineering, Cornell University, Ithaca, NY, USA

Received: 5 July 2012 – Accepted: 9 July 2012 – Published: 24 July 2012

Correspondence to: L. K. Emmons (emmons@ucar.edu)

Published by Copernicus Publications on behalf of the European Geosciences Union.

Abstract

A procedure for tagging ozone produced from NO sources through updates to an existing chemical mechanism is described, and results from its implementation in the Model for Ozone and Related chemical Tracers (MOZART-4), a global chemical transport model, are presented. Artificial tracers are added to the mechanism, thus not affecting the standard chemistry. The results are linear in the troposphere, i.e., the sum of ozone from individual tagged sources equals the ozone from all sources to within 3 % in zonal mean monthly averages. The stratospheric ozone contribution to the troposphere determined from the difference between total ozone and ozone from all tagged sources is significantly less than estimates using a traditional stratospheric ozone tracer (8 vs 20 ppbv at the surface). The commonly used technique of perturbing NO emissions by 20 % in a region to determine its ozone contribution is compared to the tagging technique, showing that the tagged ozone is 2–4 times the ozone contribution that was deduced from perturbing emissions.

1 Introduction

The transport of pollution from one region (state, country, or continent) to another has been the goal of a great number of studies due to its importance to local air quality, and consequently human health and ecosystems (e.g., Dentener et al., 2010). Global chemical transport models have been used in a variety of ways to determine source attributions at given locations, and source-receptor relationships. Pollutants such as carbon monoxide (CO), with relatively simple chemistry (i.e., directly emitted, lost through reaction with OH and dry deposition), can be easily "tagged" according to emission source types or regions for attribution studies (e.g., Granier et al., 1999; Pfister et al., 2004, 2011) or inverse modeling (e.g., Pétron et al., 2004; Arellano et al., 2006). The contribution of isoprene emissions to formaldehyde, carbon monoxide and other products was determined through a tagging technique similar to that presented here for

GMDD

5, 1949–1985, 2012

ozone, where duplicate "tagged" species were created for each carbon compound derived from isoprene (Pfister et al., 2008a). The NO_x budget was analyzed in the study of Lamarque et al. (1996) by tagging each type of NO_x source. For that study, the separate source tracers equaled the total NO_x, and the non-linearities of loss and production rates were taken into account so that the sum of the tagged tracers equalled total NO_x.

Ozone, however, has quite complex chemical production and loss processes, and is not directly emitted, so identifying its source contributions requires slightly different procedures. One method of understanding source contributions to tropospheric ozone has been to set the emissions of a given region to zero and compare the results to a standard simulation with no emission perturbation to determine the influence of that region on other regions (e.g., Fiore et al., 2002; Guerova et al., 2006). Other studies have made a small change (5–20 %) in the emissions of a region, and then scaled the resulting difference from a standard run to estimate the total impact of that region. This technique has been used by the model comparisons performed for the Task Force on Hemispheric Transport of Air Pollution (HTAP; http://www.htap.org). Analyses of these simulations have provided estimates of foreign emissions on local ozone concentrations (e.g., Fiore et al., 2009; Reidmiller et al., 2009; Wild et al., 2012). Wu et al. (2009) showed that estimates of ozone contributions are significantly different between removing and only perturbing emissions in source regions, due to the non-linearity of ozone photochemistry, indicating that a small perturbation will give a more accurate result than removing the source.

A simplified NO_x–ozone tagging scheme, suitable for long chemistry-climate simulations, has been presented by Grewe (2004). In that treatment, each NO_x source produces a NO_y tracer in addition to the standard chemical scheme. Each NO_y tracer has a corresponding ozone tracer that is produced at a fraction of the ozone production rate corresponding to the fraction of each NO_y tracer to total NO_y. This methodology was compared to the procedure of perturbing emissions as a means of estimating source contributions by Grewe et al. (2010). The contributions of NO_x sources to ozone radiative forcing trends have also been estimated (Dahlmann et al., 2011).

GMDD
5, 1949–1985, 2012

In this paper we present a technique for quantifying source contributions to tropospheric ozone distributions by "tagging" emissions of NO and its resulting products, and following them to the production of ozone. This technique adds synthetic tracers to the chemical mechanism that do not modify the original chemistry, but make use of the mixing ratios and loss rates of the full, standard chemistry. The tagging scheme presented here has been used in several studies (Lamarque et al., 2005; Pfister et al., 2006; Hess and Lamarque, 2007; Pfister et al., 2008b; Emmons et al., 2010a; Brown-Steiner and Hess, 2011; Wespes et al., 2012), but never fully documented. We present here the details of the mechanism (in Sect. 2), and illustrate the additive qualities of the technique and comparisons to other attribution techniques (Sect. 3).

2 Tagged mechanism

The method we use to attribute the ozone concentration produced by a given source type or region is through the "tagging" of nitrogen (i.e., NO, NO_2) emissions. The tagged NO_x is traced through all of the odd nitrogen species (e.g., PAN, HNO_3, organic nitrates) to account for recycling of NO_x. The photolysis of tagged NO_2 produces tagged O, most of which goes on to produce tagged O_3. Tagged O_3 is then destroyed at the same rate as total ozone. While ozone production also requires the presence of peroxy radicals (HO_2 and RO_2) resulting from the oxidation of hydrocarbons, we have chosen to trace the nitrogen species for determining ozone sources.

Table 1 lists the additional, tagged species needed to determine the tagged ozone. The photolysis and kinetic reactions for the tagged species are listed in Tables 2 and 3 along with the corresponding reactions for the non-tagged species. The tagged N species are indicated by XN, while the tagged O_x species end in A (e.g., O3A) For the tagged reactions, any non-tagged species among the reactants are included as products in each reaction, so that their concentration is not affected by the tagged species. Similarly, the non-tagged products are not included in the tagged reaction. For example, the standard reaction $NO + HO_2$ produces $NO_2 + OH$. In the tagged reaction,

GMDD
5, 1949–1985, 2012

tagged NO goes to tagged NO_2 using the current HO_2 concentration, but the HO_2 is unchanged by the reaction, and no additional OH is produced (see Table 3). Therefore, oxidant levels and non-tagged species are unchanged and the photochemistry occurs just as if the tagging were not included. There are a few reactions that are nonlinear in nitrogen species, such as $NO_2 + NO_3$, so the combination of tagged and non-tagged nitrogen must be considered (as discussed in Lamarque et al., 1996). As shown in Table 3, there are two tagged reactions for $NO_2 + NO_3 + M \rightarrow N_2O_5 + M$:

$$XNO_2 + NO_3 + M \rightarrow XNO_2NO_3 + NO_3 + M$$
$$NO_2 + XNO_3 + M \rightarrow NO_2XNO_3 + NO_2 + M$$

The tagged species are operated on by wet and dry deposition at the same rate as their non-tagged counterparts. Tagged ozone, NO and NO_2 are relaxed to zero in the stratosphere on a timescale of ten days.

3 Results

The results presented here are from simulations of MOZART-4 (Emmons et al., 2010b) for 2008, after a 6-month spin-up for each tagging simulation. The meteorological fields used to drive MOZART-4 for this study are from the NASA Global Modeling and Assimilation Office (GMAO) GEOS-5 assimilation products (http://gmao.gsfc.nasa.gov/products/). The emissions are the same as used in Wespes et al. (2012), with anthropogenic emissions from D. Streets' ARCTAS inventory (see http://www.cgrer.uiowa.edu/arctas/emission.html), which is based on Zhang et al. (2009), and fire emissions from the Fire Inventory from NCAR, (FINN, Wiedinmyer et al., 2011).

NO emissions are included for surface anthropogenic sources (including fossil fuel and biofuel combustion), open fire burning, from soil, lightning and aircraft. Soil emissions include a contribution from fertilizer, with the natural source calculated online based on soil moisture (cf., Emmons et al., 2010b). Lightning emissions are also calculated online in the model, using the Price et al. (1997) parameterization dependent

GMDD
5, 1949–1985, 2012

on cloud height (see Emmons et al., 2010b, for details). Aircraft emissions are emitted as a 3-D field with monthly variation (Emmons et al., 2010b). Table 4 gives the monthly global NO emissions for each sector. The majority of the emissions, by far, are from anthropogenic surface sources. However, away from urban areas, and in the free troposphere, the other sources can be locally very important for ozone production.

3.1 Tropospheric sources

Figures 1 and 2 show maps of the tropospheric column of each tagged ozone contribution (anthropogenic surface sources, fires, soil, lightning, aircraft and the stratosphere) for January and July 2008. For this analysis, we use a chemical tropopause defined as the altitude where ozone reaches 150 ppbv (e.g., Stevenson et al., 2006). The surface anthropogenic emissions are the largest contribution in the Northern Hemisphere in both seasons, while lightning is the dominant source in the Tropics. The location of fire emissions changes with season, with the savanna region of northern Tropical Africa having the strongest contribution in January. In July, the tropical regions of South America and Africa have notable ozone contributions from agricultural fires, with the large wildfires in Siberia and Canada also evident. The contribution from soil NO emissions are most apparent in the summer season of each hemisphere, while the stratospheric contribution is largest in winter.

Figures 3 and 4 show the vertical distribution of each ozone contribution. In January, anthropogenic surface sources are maximum in the lower and mid troposphere of the Northern Hemisphere (NH), while in July strong summertime convection distributes its ozone contribution throughout the troposphere at mid-latitudes. A similar summer-winter pattern is seen in the Southern Hemisphere (SH), but the anthropogenic sources are so much smaller there, the ozone contribution is much less. The vertical distribution of the ozone contributions from fires and soil emissions shows the seasonal variation in both the sources and convection and transport patterns. Lightning and aircraft emissions originate in the upper troposphere, with aircraft activity largest in the NH and lightning peaking in the tropics and in summer at mid-latitudes. While lightning

GMDD
5, 1949–1985, 2012

produces only NO (at least in the model), sufficient concentrations of CO and VOCs are transported within the convective systems to lead to large amounts of ozone production (e.g., Hauglustaine et al., 2001). Aircraft have very low CO and hydrocarbon emissions coincident with NO, but background levels of CO and VOCs are sufficient for ozone production in the upper troposphere, resulting in up to 30 ppbv ozone contribution in the zonal average in July. The stratospheric ozone contribution clearly shows the level of the tropopause approximately at the 100 ppbv contour, with highest values in the troposphere in the winter hemisphere.

Figure 5 shows zonal averages for each season (1-month average) of the contributions of ozone at the surface from each NO source type. As seen in the previous figures, the anthropogenic contribution is dominant in the Northern Hemisphere for all seasons. In the Southern Hemisphere, lightning and stratospheric air are a larger fraction of the total ozone. Biomass burning has a large seasonal variation, however with a relatively small contribution to the total. Soil emissions peak in the summer mid-latitudes of both hemispheres. Figure 6 similarly shows the ozone amounts for different sources at 400 hPa, with very different relative contributions than at the surface. Lightning is the largest contribution in the Tropics and sub-Tropics. The stratospheric contribution is most significant in NH winter and spring. Anthropogenic emissions are the source for twice as much ozone in the NH than the SH, but contribute a smaller fraction than at the surface. The small white area in Fig. 6 between the contributions from lightning and the stratosphere indicates the difference between the sum of the individually tagged sources and the result from tagging all sources at once. This shows the level of non-linearity in the method and corresponds to 3 % or less in the zonal average at 400 hPa, and less than 1 % at the surface.

The same source contributions to NO_x, PAN and HNO_3 at 400 hPa are shown in Figs. 7, 8 and 9. As for ozone, the most important contributions are from anthropogenic and lightning emissions for all three of these species. The stratospheric source for these compounds is determined in the same manner as for ozone (the difference between simulated total of the species and the contribution from all tropospheric sources

GMDD
5, 1949–1985, 2012

tagged). For NO_x, the stratospheric contribution is barely noticeable in these plots, but for HNO_3 it is important, and for the SH winter is essentially the only source south of 50° S.

HNO_3 shows the largest missing contribution between the sum of individual source tags and all sources (the white area in the plot between the lightning and stratosphere contributions). This is due to the non-linearity of wet deposition and HNO_3 is much more soluble than the other reactive nitrogen compounds. The washout rate for the tagged HNO_3 is the same as for total HNO_3, but the amount of tagged HNO_3 will be limited by the available mass of that tag. So, at times (and places) all of the mass of a HNO_3 tag may be removed from the atmosphere, eliminating any possibility of recycling to NO_2 (through photolysis) and reformation of HNO_3.

3.2 Stratospheric ozone

One commonly studied source of ozone is the stratospheric contribution to the troposphere. Many modeling studies have used a tracer ("O3S") that is set to the ozone mixing ratio in the stratosphere and is destroyed below the tropopause at the same rate as ozone (e.g., Roelofs and Lelieveld, 1997; Wang et al., 1998; Emmons et al., 2003). This technique however gives an upper limit to the stratospheric ozone contribution, as tropospheric air that is transported into the stratosphere is reset to the stratospheric value. By tagging all of the tropospheric sources (surface anthropogenic, biomass burning, soil, lightning, and aircraft emissions), we can determine the amount of ozone produced from tropospheric sources, and thus the stratospheric contribution from the difference of the tagged amount and the total ozone.

Figure 10 shows the stratospheric contribution determined from the tagged tropospheric sources, as well as from the traditional "O3S" tracer. The O3S tracer gives a much greater estimate of stratospheric ozone than the tagged ozone does, both in the mid-troposphere and at the surface. At the surface, where O3S shows over 20 ppbv, the tagged ozone gives no more than 8 ppbv. Hess and Lamarque (2007) showed similar differences in zonal averages of surface O3S and tagged ozone. When considering

GMDD
5, 1949–1985, 2012

the whole troposphere (ozone less than 150 ppbv), the fraction of the tropospheric ozone burden that is from the stratosphere is 58 % based on O3S, and 17 % based on the tagged ozone. These differences are comparable to those found using different measures by Emmons et al. (2003) in an analysis of the Northern Hemisphere springtime ozone increase.

3.3 Comparison to perturbed source attribution

Simulations with perturbed emissions are primarily used to quantify the impacts of changes in emissions scenarios, but have also been used to approximate total source contributions. As mentioned above, many previous studies have determined ozone contributions from source regions by decreasing the NO emissions of that region and scaling the difference between the perturbed run and a standard run (e.g., Fiore et al., 2009; Reidmiller et al., 2009). We have performed a test simulation in this manner with NO emissions in Asia reduced by 20 %, so as to compare it with our method of tagging NO. Figure 11 shows the original NO surface emissions (shipping, anthropogenic, fires and soil) for May 2008, also indicating the Asian region that has been either tagged or perturbed. This region is roughly the combination of the South Asia and East Asia regions used in the HTAP simulations (e.g., Fiore et al., 2009). Figure 12 shows a comparison of surface ozone attributed to emissions in Asia using these two techniques for several receptor regions (the N. America and Europe regions are similar to, but not exactly the same as, the HTAP regions). The two methods give notably different results. Over Asia, the average surface ozone produced from sources in Asia is 20–25 ppbv in the Tagged method, but 1–6 ppbv in the Perturbed method. The seasonal cycle is also different, with the Tagged method peaking in April and having a minimum in August, while the Perturbed method shows a broad summer maximum. In the downwind regions, the seasonal cycle is more similar in the two methods, with the magnitude of the differences decreasing while progressing from the northeast Pacific to North America to Europe.

GMDD
5, 1949–1985, 2012

The results from the simulations with perturbed emissions agree well with the results of the HTAP simulations presented in Fig. 11 of Fiore et al. (2009). In the HTAP results, the estimated contribution of East Asia in North America is about 1.5 ppbv in spring and less than 1 ppbv in summer. This matches our results for the Perturbed case in the N. America panel of Fig. 12. Brown-Steiner and Hess (2011) found a similar difference between the HTAP results and their simulations with CAM-chem using the same tagged ozone procedure as presented here. That study found tagged ozone from Asia at the surface in North America to be 2–2.5 times that determined by the HTAP perturbed attribution procedure.

Although a perturbation of 20 % in the emissions may seem small, it can have a significant impact on the local chemistry. Figs. 13–15 show the impact of the perturbation on several species at the surface for the May monthly average. At the surface, there is little change in NO_x mixing ratios outside the perturbed region, due to its short lifetime (Fig. 13, top panel). The horizontal distribution of the change in O_3 (Fig. 13, bottom panel) shows the ozone increases (about 5 %) over the high NO_x emission regions of northeast China (including Beijing and Shanghai), while decreasing up to 10 % over Southeast Asia but only about 2 % over the eastern Pacific Ocean. Fig. 14 shows the striking difference in the response of OH and HO_2 to the change in NO emissions. Over Asia, OH is reduced by 10–20 %, except over Beijing and Shanghai, a result of the decrease of OH production from $NO + HO_2$. HO_2 is higher in the perturbed case by up to 20 % in northeastern China, but elsewhere is lower by 1–5 %.

The changes in the ozone production and loss rates are shown in Fig. 15. The ozone production rate shown here is determined from the rate-limiting steps, $NO + HO_2$ and $NO + RO_2$, so the change in the rate is primarily due to the change in the NO mixing ratio. The ozone loss rate depends on the ozone concentration, with the most significant terms (aside from photolysis of ozone) being $OH + O_3$, $HO_2 + O_3$ and $O_1D + H_2O$. Thus, the nonlinear response in OH and HO_2 due to a change in NO is reflected in the nonlinear response in ozone.

GMDD
5, 1949–1985, 2012

4 Conclusions

A technique of tagging ozone from various source regions by using artificial tracers of NO and its oxidation products has been described. This method shows a high degree of linearity: the sum of tagged ozone from individual sources is equal to the tagged ozone of all sources, within 3 % in zonal averages in the troposphere. This tagging procedure allows source contributions to NO_x products, such as PAN and HNO_3, to be quantified as well. Comparisons to other standard attribution methods show significant differences. The contribution of stratospheric ozone to the troposphere using this tagging method is significantly lower than estimates using a stratospheric ozone tracer. In comparison to determining source contributions by perturbing NO emissions, the tagging method gives significantly higher contributions, at least for an example for Asia emissions. These differences are due to the non-linearity of ozone chemistry, where both ozone production and loss rates are affected by a change in NO concentrations.

The mechanism file and source code modifications for MOZART-4 and CAM-chem are available from the authors.

Acknowledgements. The GEOS-5 data used in this study have been provided by the Global Modeling and Assimilation Office (GMAO) at NASA Goddard Space Flight Center. The National Center for Atmospheric Research is funded by the National Science Foundation.

References

Arellano, A. F., Kasibhatla, P. S., Giglio, L., van der Werf, G. R., Randerson, J. T., and Collatz, G. J.: Time-dependent inversion estimates of global biomass-burning CO emissions using Measurement of Pollution in the Troposphere (MOPITT) measurements, J. Geophys. Res., 111, D09303, doi:10.1029/2005JD006613, 2006. 1950

Brown-Steiner, B. and Hess, P.: Asian influence on surface ozone in the United States: A comparison of chemistry, seasonality, and transport mechanisms, J. Geophys. Res., 116, D17309, doi:10.1029/2011JD015846, 2011. 1952, 1958

GMDD

5, 1949–1985, 2012

Dahlmann, K., Grewe, V., Ponater, M., and Matthes, S.: Quantifying the contributions of individual NO_x sources to the trend in ozone radiative forcing, Atmos. Environ., 45, 2860–2868, 2011. 1951

Dentener, F., Keating, T., and Akimoto, H. (Eds.): Hemispheric Transport of Air Pollution, United Nations, available at: http://htap.org (last access: January 2012), 2010. 1950

Emmons, L., Hess, P., Klonecki, A., Tie, X., Horowitz, L., Lamarque, J. F., Kinnison, D., Brasseur, G., Atlas, E., Browell, E., Cantrell, C., Eisele, F., Mauldin, R. L., Merrill, J., Ridley, B., and Shetter, R.: Budget of tropospheric ozone during TOPSE from two chemical transport models, J. Geophys. Res., 108, 8372, doi:10.1029/2002JD002665, 2003. 1956, 1957

Emmons, L. K., Apel, E. C., Lamarque, J.-F., Hess, P. G., Avery, M., Blake, D., Brune, W., Campos, T., Crawford, J., DeCarlo, P. F., Hall, S., Heikes, B., Holloway, J., Jimenez, J. L., Knapp, D. J., Kok, G., Mena-Carrasco, M., Olson, J., O'Sullivan, D., Sachse, G., Walega, J., Weibring, P., Weinheimer, A., and Wiedinmyer, C.: Impact of Mexico City emissions on regional air quality from MOZART-4 simulations, Atmos. Chem. Phys., 10, 6195–6212, doi:10.5194/acp-10-6195-2010, 2010a. 1952

Emmons, L. K., Walters, S., Hess, P. G., Lamarque, J.-F., Pfister, G. G., Fillmore, D., Granier, C., Guenther, A., Kinnison, D., Laepple, T., Orlando, J., Tie, X., Tyndall, G., Wiedinmyer, C., Baughcum, S. L., and Kloster, S.: Description and evaluation of the Model for Ozone and Related chemical Tracers, version 4 (MOZART-4), Geosci. Model Dev., 3, 43–67, doi:10.5194/gmd-3-43-2010, 2010b. 1953, 1954

Fiore, A. M., Jacob, D. J., Bey, I., Yantosca, R. M., Field, B. D., Fusco, A. C., and Wilkinson, J. G.: Background ozone over the United States in summer: origin, trend, and contribution to pollution episodes, J. Geophys. Res., 107, D15, doi:10.1029/2001JD000982, 2002. 1951

Fiore, A. M., Dentener, F. J., Wild, O., et al.: Multimodel estimates of intercontinental source-receptor relationships for ozone pollution, J. Geophys. Res., 114, D04301, doi:10.1029/2008JD010816, 2009. 1951, 1957, 1958

Granier, C., Müller, J.-F., Pétron, G., and Brasseur, G.: A three-dimensional study of the global CO budget, Chemosphere Glob. Change Sci., 1, 255–261, 1999. 1950

Grewe, V.: Technical Note: A diagnostic for ozone contributions of various NO_x emissions in multi-decadal chemistry-climate model simulations, Atmos. Chem. Phys., 4, 729–736, doi:10.5194/acp-4-729-2004, 2004. 1951

GMDD

5, 1949–1985, 2012

Grewe, V., Tsati, E., and Hoor, P.: On the attribution of contributions of atmospheric trace gases to emissions in atmospheric model applications, Geosci. Model Dev., 3, 487–499, doi:10.5194/gmd-3-487-2010, 2010. 1951

Guerova, G., Bey, I., Attié, J.-L., Martin, R. V., Cui, J., and Sprenger, M.: Impact of transatlantic transport episodes on summertime ozone in Europe, Atmos. Chem. Phys., 6, 2057–2072, doi:10.5194/acp-6-2057-2006, 2006. 1951

Hauglustaine, D., Emmons, L., Newchurch, M., Brasseur, G., Takao, T., Matsubara, K., Johnson, J., Ridley, B., Stith, J., and Dye, J.: On the role of lightning NO_x in the formation of tropospheric ozone plumes: a global model perspective, J. Atmos. Chem., 38, 277–294, doi:10.1023/A:1006452309388, 2001. 1955

Hess, P. G. and Lamarque, J.-F.: Ozone source attribution and its modulation by the Arctic oscillation during the spring months, J. Geophys. Res., 112, D11303, doi:10.1029/2006JD007557, 2007. 1952, 1956

Lamarque, J.-F., Brasseur, G. P., Hess, P. G., and Müller, J.-F.: Three-dimensional study of the relative contributions of the different nitrogen sources in the troposphere, J. Geophys. Res., 101, 22, 955–968, 1996. 1951, 1953

Lamarque, J.-F., Hess, P., Emmons, L., Buja, L., Washington, W., and Granier, C.: Tropospheric ozone evolution between 1890 and 1990, J. Geophys. Res., 110, D08304, doi:10.1029/2004JD005537, 2005. 1952

Pétron, G., Granier, C., Khattotov, B., Yudin, V., Lamarque, J.-F., Emmons, L., Gille, J., and Edwards, D. P.: Monthly CO surface sources inventory based on the 2000–2001 MOPITT satellite data, Geophys. Res. Lett., 31, L21107, doi:10.1029/2004GL020560, 2004. 1950

Pfister, G., Pétron, G., Emmons, L. K., Gille, J. C., Edwards, D. P., Lamarque, J.-F., Attié, J.-L., Granier, C., and Novelli, P. C.: Evaluation of CO simulations and the analysis of the CO budget for Europe, J. Geophys. Res., 109, D19304, doi:10.1029/2004JD004691, 2004. 1950

Pfister, G. G., Emmons, L. K., Hess, P. G., Honrath, R., Lamarque, J.-F., Martin, M., Val and Owen, R. C., Avery, M. A., Browell, E. V., Holloway, J. S., Nedelec, P., Purvis, R., Ryerson, T. B., Sachse, G. W., and Schlager, H.: Ozone production from the 2004 North American boreal fires, J. Geophys. Res., 111, D24S07, doi:10.1029/2006JD007695, 2006. 1952

Pfister, G. G., Emmons, L. K., Hess, P. G., Lamarque, J.-F., Orlando, J. J., Walters, S., Guenther, A., Palmer, P. I., and Lawrence, P. J.: Contribution of isoprene to chemical budgets: a model tracer study with the NCAR CTM MOZART-4, J. Geophys. Res., 113, D05308, doi:10.1029/2007JD008948, 2008a. 1951

GMDD

5, 1949–1985, 2012

Pfister, G. G., Emmons, L. K., Hess, P. G., Lamarque, J.-F., Thompson, A. M., and Yorks, J. E.: Analysis of the Summer 2004 ozone budget over the United States using Intercontinental Transport Experiment Ozonesonde Network Study (IONS) observations and Model of Ozone and Related Tracers (MOZART-4) simulations, J. Geophys. Res., 113, D23306, doi:10.1029/2008JD010190, 2008b. 1952

Pfister, G. G., Avise, J., Wiedinmyer, C., Edwards, D. P., Emmons, L. K., Diskin, G. D., Podolske, J., and Wisthaler, A.: CO source contribution analysis for California during ARCTAS-CARB, Atmos. Chem. Phys., 11, 7515–7532, doi:10.5194/acp-11-7515-2011, 2011. 1950

Price, C., Penner, J., and Prather, M.: NO_x from lightning 1. Global distribution based on lightning physics, J. Geophys. Res., 102, 5929–5941, 1997. 1953

Reidmiller, D. R., Fiore, A. M., Jaffe, D. A., Bergmann, D., Cuvelier, C., Dentener, F. J., Duncan, B. N., Folberth, G., Gauss, M., Gong, S., Hess, P., Jonson, J. E., Keating, T., Lupu, A., Marmer, E., Park, R., Schultz, M. G., Shindell, D. T., Szopa, S., Vivanco, M. G., Wild, O., and Zuber, A.: The influence of foreign vs. North American emissions on surface ozone in the US, Atmos. Chem. Phys., 9, 5027–5042, doi:10.5194/acp-9-5027-2009, 2009. 1951, 1957

Roelofs, G.-J. and Lelieveld, J.: Model study of the influence of cross-tropopause O_3 transports on tropospheric O_3 levels, Tellus B, 49, 38–55, 1997. 1956

Stevenson, D. S., Dentener, F., Schultz, M., et al.: Multimodel ensemble simulations of present-day and near-future tropospheric ozone, J. Geophys. Res., 111, D08301, doi:10.1029/2005JD006338, 2006. 1954

Wang, Y., Jacob, D. J., and Logan, J. A.: Global simulation of tropospheric O_3-NO_x -hydrocarbon chemistry, 3, Origin of tropospheric ozone and effects of nonmethane hydrocarbons, J. Geophys. Res., 103, 10757–10767, 1998. 1956

Wespes, C., Emmons, L., Edwards, D. P., Hannigan, J., Hurtmans, D., Saunois, M., Coheur, P.-F., Clerbaux, C., Coffey, M. T., Batchelor, R. L., Lindenmaier, R., Strong, K., Weinheimer, A. J., Nowak, J. B., Ryerson, T. B., Crounse, J. D., and Wennberg, P. O.: Analysis of ozone and nitric acid in spring and summer Arctic pollution using aircraft, ground-based, satellite observations and MOZART-4 model: source attribution and partitioning, Atmos. Chem. Phys., 12, 237–259, doi:10.5194/acp-12-237-2012, 2012. 1952, 1953

Wiedinmyer, C., Akagi, S. K., Yokelson, R. J., Emmons, L. K., Al-Saadi, J. A., Orlando, J. J., and Soja, A. J.: The Fire INventory from NCAR (FINN): a high resolution global model to estimate

GMDD
5, 1949–1985, 2012

the emissions from open burning, Geosci. Model Dev., 4, 625–641, doi:10.5194/gmd-4-625-2011, 2011. 1953

Wild, O., Fiore, A. M., Shindell, D. T., Doherty, R. M., Collins, W. J., Dentener, F. J., Schultz, M. G., Gong, S., MacKenzie, I. A., Zeng, G., Hess, P., Duncan, B. N., Bergmann, D. J., Szopa, S., Jonson, J. E., Keating, T. J., and Zuber, A.: Modelling future changes in surface ozone: a parameterized approach, Atmos. Chem. Phys., 12, 2037–2054, doi:10.5194/acp-12-2037-2012, 2012. 1951

Wu, S., Duncan, B. N., Jacob, D. J., Fiore, A. M., and Wild, O.: Chemical nonlinearities in relating intercontinental ozone pollution to anthropogenic emissions, Geophys. Res. Lett., 36, L05806, doi:10.1029/2008GL036607, 2009. 1951

Zhang, Q., Streets, D. G., Carmichael, G. R., He, K. B., Huo, H., Kannari, A., Klimont, Z., Park, I. S., Reddy, S., Fu, J. S., Chen, D., Duan, L., Lei, Y., Wang, L. T., and Yao, Z. L.: Asian emissions in 2006 for the NASA INTEX-B mission, Atmos. Chem. Phys., 9, 5131–5153, doi:10.5194/acp-9-5131-2009, 2009. 1953

GMDD

5, 1949–1985, 2012

Table 1. Tagged species in the MOZART-4 tagged ozone mechanism.

Symbolic name	Atomic composition
XNO	NO
XNO2	NO_2
XNO3	NO_3
XHNO3	HNO_3
XHO2NO2	HNO_4
XNO2NO3	N_2O_5
NO2XNO3	N_2O_5
XPAN	$CH_3CO_3NO_2$
XONIT	$CH_3COCH_2ONO_2$
XMPAN	$CH_2CCH_3CO_3NO_2$
XISOPNO3	$CH_2CHCCH_3OOCH_2ONO_2$
XONITR	$CH_2CCH_3CHONO_2CH_2OH$
XNH4NO3	NH_4NO_3
OA	O
O1DA	O
O3A	O_3

GMDD
5, 1949–1985, 2012

Table 2. Photolysis reactions of tagged species.

Original reaction			Tagged reaction(s)		
O3 + hν	→	O1D + O2	O3A + hν	→	O1DA
O3 + hν	→	O + O2	O3A + hν	→	OA
NO2 + hν	→	NO + O	XNO2 + hν	→	XNO + OA
N2O5 + hν	→	NO2 + NO3	XNO2NO3 + hν	→	XNO2
			NO2XNO3 + hν	→	XNO3
HNO3 + hν	→	NO2 + OH	XHNO3 + hν	→	XNO2
NO3 + hν	→	.89*NO2 + .11*NO + .89*O3	XNO3 + hν	→	.89*XNO2 + .11*XNO + .89*O3A
HO2NO2 + hν	→	.33*OH + .33*NO3 + .66*NO2 + .66*HO2	XHO2NO2 + hν	→	.33*XNO3 + .66*XNO2
PAN + hν	→	.6*CH3CO3 + .6*NO2 + .4*CH3O2 + .4*NO3	XPAN + hν	→	.6*XNO2 + .4*XNO3
MPAN + hν	→	MCO3 + NO2	XMPAN + hν	→	XNO2
ONITR + hν	→	HO2 + CO + NO2 + CH2O	XONITR + hν	→	XNO2

GMDD
5, 1949–1985, 2012

Table 3. Gas-phase reactions of tagged species.

Original reaction			Tagged reaction(s)		
O + O2 + M	→	O3 + M	OA + O2 + M	→	O3A + M
O + O3	→	2*O2	OA + O3	→	O3
			O + O3A	→	O
O1D + N2	→	O + N2	O1DA + N2	→	OA + N2
O1D + O2	→	O + O2	O1DA + O2	→	OA + O2
O1D + H2O	→	2*OH	O1DA + H2O	→	H2O
H2 + O1D	→	HO2 + OH	H2 + O1DA	→	H2
O + OH	→	HO2 + O2	OA + OH	→	OH
HO2 + O	→	OH + O2	HO2 + OA	→	HO2
OH + O3	→	HO2 + O2	OH + O3A	→	OH
HO2 + O3	→	OH + 2*O2	HO2 + O3A	→	HO2
N2O + O1D	→	N2 + O2	N2O + O1DA	→	N2O
N2O + O1D	→	2*NO	N2O + O1DA	→	N2O
NO + HO2	→	NO2 + OH	XNO + HO2	→	XNO2 + HO2
NO + O3	→	NO2 + O2	XNO + O3	→	XNO2 + O3
			NO + O3A	→	NO
NO2 + O	→	NO + O2	XNO2 + O	→	XNO + O
			NO2 + OA	→	NO2
NO2 + O3	→	NO3 + O2	XNO2 + O3	→	XNO3 + O3
			NO2 + O3A	→	NO2
NO3 + HO2	→	OH + NO2	XNO3 + HO2	→	HO2 + XNO2
NO2 + NO3 + M	→	N2O5 + M	XNO2 + NO3 + M	→	XNO2NO3 + NO3 + M
			NO2 + XNO3 + M	→	NO2XNO3 + NO2 + M
N2O5 + M	→	NO2 + NO3 + M	XNO2NO3 + M	→	XNO2 + M
			NO2XNO3 + M	→	XNO3 + M
NO2 + OH + M	→	HNO3 + M	XNO2 + OH + M	→	XHNO3 + OH + M
HNO3 + OH	→	NO3 + H2O	XHNO3 + OH	→	XNO3 + OH
NO3 + NO	→	2*NO2	XNO3 + NO	→	XNO2 + NO
			NO3 + XNO	→	XNO2 + NO3
NO2 + HO2 + M	→	HO2NO2 + M	XNO2 + HO2 + M	→	XHO2NO2 + HO2 + M
HO2NO2 + OH	→	H2O + NO2 + O2	XHO2NO2 + OH	→	XNO2 + OH
HO2NO2 + M	→	HO2 + NO2 + M	XHO2NO2 + M	→	XNO2 + M
CH4 + O1D	→	.75*CH3O2 + .75*OH + .25*CH2O + .4*HO2 + .05*H2	CH4 + O1DA	→	CH4
CH3O2 + NO	→	CH2O + NO2 + HO2	CH3O2 + XNO	→	CH3O2 + XNO2
CH2O + NO3	→	CO + HO2 + HNO3	CH2O + XNO3	→	CH2O + XHNO3
C2H4 + O3	→	CH2O + .12*HO2 + .5*CO + .12*OH + .25*CH3COOH	C2H4 + O3A	→	C2H4

GMDD
5, 1949–1985, 2012

Table 3. Continued.

Original reaction			Tagged reaction(s)		
EO2 + NO	→	EO + NO2	EO2 + XNO	→	EO2 + XNO2
C2H5O2 + NO	→	CH3CHO + HO2 + NO2	C2H5O2 + XNO	→	C2H5O2+ XNO2
CH3CHO + NO3	→	CH3CO3 + HNO3	CH3CHO + XNO3	→	CH3CHO + XHNO3
CH3CO3 + NO	→	CH3O2 + NO2	CH3CO3 + XNO	→	CH3CO3 + XNO2
CH3CO3 + NO2 + M	→	PAN + M	CH3CO3 + XNO2 + M	→	XPAN + CH3CO3 + M
PAN + OH	→	CH2O + NO3	XPAN + OH	→	XNO3 + OH
PAN + M	→	CH3CO3 + NO2 + M	XPAN + M	→	XNO2 + M
C3H6 + O3	→	.54*CH2O + .19*HO2 + .33*OH + .5*CH3CHO + .56*CO + .31*CH3O2 + .25*CH3COOH + .08*CH4	C3H6 + O3A	→	C3H6
C3H6 + NO3	→	ONIT	C3H6 + XNO3	→	C3H6 + XONIT
PO2 + NO	→	CH3CHO + CH2O + HO2 + NO2	PO2 + XNO	→	PO2 + XNO2
C3H7O2 + NO	→	.82*CH3COCH3 + NO2 + .27*CH3CHO + HO2	C3H7O2 + XNO	→	C3H7O2 + XNO2
RO2 + NO	→	CH3CO3 + CH2O + NO2	RO2 + XNO	→	RO2 + XNO2
ONIT + OH	→	NO2 + CH3COCHO	XONIT + OH	→	XNO2 + OH
CH3COCHO + NO3	→	HNO3 + CO + CH3CO3	CH3COCHO + XNO3	→	XHNO3 + CH3COCHO
ENEO2 + NO	→	CH3CHO + .5*CH2O + .5*CH3COCH3 + HO2 + NO2	ENEO2 + XNO	→	ENEO2 + XNO2
MEKO2 + NO	→	CH3CO3 + CH3CHO + NO2	MEKO2 + XNO	→	MEKO2 + XNO2
MPAN + OH + M	→	.5*HYAC + .5*NO3 + .5*CH2O + .5*HO2 + M	XMPAN + OH + M	→	.5*XNO3 + OH + M
ALKO2 + NO	→	.4*CH3CHO + .1*CH2O + .25*CH3COCH3 + .9*HO2 + .75*MEK + .9*NO2 + .1*ONIT	ALKO2 + XNO	→	ALKO2 + .9*XNO2 + .1*XONIT
ISOP + O3	→	.4*MACR + .2*MVK + .07*C3H6 + .27*OH + .06*HO2 + .6*CH2O + .3*CO + .1*O3 + .2*MCO3 + .2*CH3COOH	ISOP + O3A	→	ISOP + .1*O3A
ISOPO2 + NO	→	.08*ONITR + .92*NO2 + HO2 + .55*CH2O + .23*MACR + .32*MVK + .37*HYDRALD	ISOPO2 + XNO	→	ISOPO2 + .08*XONITR + .92*XNO2
ISOPO2 + NO3	→	HO2 + NO2 + .6*CH2O + .25*MACR + .35*MVK + .4*HYDRALD	ISOPO2 + XNO3	→	ISOPO2 + XNO2

GMDD
5, 1949–1985, 2012

Table 3. Continued.

Original reaction			Tagged reaction(s)		
ISOP + NO3	→	ISOPNO3	ISOP + XNO3	→	ISOP + XISOPNO3
ISOPNO3 + NO	→	1.206*NO2 + .072*CH2O + .167*MACR + .039*MVK + .794*ONITR + .794*HO2	XISOPNO3 + NO ISOPNO3 + XNO	→ →	.206*XNO2 + .794*XONITR + NO 1.000*XNO2 + ISOPNO3
ISOPNO3 + NO3	→	1.206*NO2 + .072*CH2O + .167*MACR + .039*MVK + .794*ONITR + .794*HO2	XISOPNO3 + NO3 ISOPNO3 + XNO3	→ →	.206*XNO2 + .794*XONITR + NO3 1.000*XNO2 + ISOPNO3
ISOPNO3 + HO2	→	.206*NO2 + .008*CH2O + .167*MACR + .039*MVK + .794*ONITR + .794*HO2	ISOPNO3 + HO2	→	.206*XNO2 + ISOPNO3
MVK + O3	→	.8*CH2O + .95*CH3COCHO + .08*OH + .2*O3 + .06*HO2 + .05*CO + .04*CH3CHO	MVK + O3A	→	MVK + .2*O3A
MACR + O3	→	.8*CH3COCHO + .275*HO2 + .2*CO + .2*O3 + .7*CH2O + .215*OH	MACR + O3A	→	MACR + .2*O3A
MACRO2 + NO	→	NO2 + .47*HO2 + .25*CH2O + .25*CH3COCHO + .53*CH3CO3 + .53*GLYALD + .22*HYAC + .22*CO	MACRO2 + XNO	→	XNO2 + MACRO2
MACRO2 + NO MACRO2 + NO3	→ →	0.8*ONITR NO2 + .53*GLYALD + .22*HYAC + .53*CH3CO3 + .25*CH2O + .22*CO + .25*CH3COCHO + .47*HO2	MACRO2 + XNO MACRO2 + XNO3	→ →	0.8*XONITR + MACRO2 XNO2 + MACRO2
MCO3 + NO MCO3 + NO3 MCO3 + NO2 + M MPAN + M ONITR + OH ONITR + NO3	→ → → → → →	NO2 + CH2O + CH3CO3 NO2 + CH2O + CH3CO3 MPAN + M MCO3 + NO2 + M HYDRALD + .4*NO2 + HO2 HYDRALD + NO2 + HO2	MCO3 + XNO MCO3 + NO3 MCO3 + XNO2 + M XMPAN + M XONITR + OH XONITR + NO3 ONITR + XNO3	→ → → → → → →	XNO2 + MCO3 XNO2 + MCO3 XMPAN + MCO3 + M XNO2 + M .4*XNO2 + OH .5*XNO2 + NO3 .5*XNO2 + ONITR

GMDD
5, 1949–1985, 2012

Table 3. Continued. Reactions labeled (het) occur on aerosols.

Original reaction			Tagged reaction(s)		
XO2 + NO	→	NO2 + 1.5*HO2 + CO + .25*CH3COCHO + .25*HYAC + .25*GLYALD	XO2 + XNO	→	XNO2 + XO2
XO2 + NO3	→	NO2 + 1.5*HO2 + CO + .25*CH3COCHO + .25*HYAC + .25*GLYALD	XO2 + XNO3	→	XNO2 + XO2
XOH + NO2	→	.7*NO2 + .7*BIGALD + .7*HO2	XOH + XNO2	→	XOH + .7*XNO2
TOLO2 + NO	→	.45*GLYOXAL + .45*CH3COCHO + .9*BIGALD + .9*NO2 + .9*HO2	TOLO2 + XNO	→	TOLO2 + .9*NO2
C10H16 + O3	→	.7*OH + MVK + MACR + HO2	C10H16 + O3A	→	C10H16
C10H16 + NO3	→	TERPO2 + NO2	C10H16 + XNO3	→	C10H16 + XNO2
TERPO2 + NO	→	.1*CH3COCH3 + HO2 + MVK + MACR + NO2	TERPO2 + XNO	→	TERPO2 + XNO2
DMS + NO3	→	SO2 + HNO3	DMS + XNO3	→	DMS + XHNO3
N2O5	→	HNO3 (het)	XNO2NO3	→	XHNO3 (het)
			NO2XNO3	→	XHNO3 (het)
NO3	→	HNO3 (het)	XNO3	→	XHNO3 (het)
NO2	→	.5*NO + .5*HNO3 (het)	XNO2	→	.5*XNO + .5*XHNO3 (het)

GMDD
5, 1949–1985, 2012

Table 4. NO emissions used in this study (global totals in Tg yr^{-1}).

Sector	Jan	Feb	Mar	Apr	May	Jun	Jul	Aug	Sep	Oct	Nov	Dec	Annual Avg
Anthropogenic	69.9	69.9	69.9	69.9	69.9	69.9	69.9	69.9	69.9	69.9	69.9	69.9	69.9
Fires	3.4	4.4	6.4	9.0	3.5	4.5	6.1	7.8	7.9	4.1	2.9	2.6	5.2
Soil	7.3	6.9	8.4	10.5	13.1	14.2	15.5	14.6	11.6	9.6	7.9	7.3	10.6
Lightning	6.2	5.8	5.8	6.4	6.6	7.0	7.3	7.8	7.0	6.4	6.0	5.8	6.5
Aircraft	1.3	1.3	1.3	1.3	1.3	1.4	1.4	1.4	1.4	1.4	1.3	1.3	1.3
Total	88.1	88.3	91.8	97.1	94.4	97	100.2	101.5	97.8	91.4	88	86.9	93.5

GMDD
5, 1949–1985, 2012

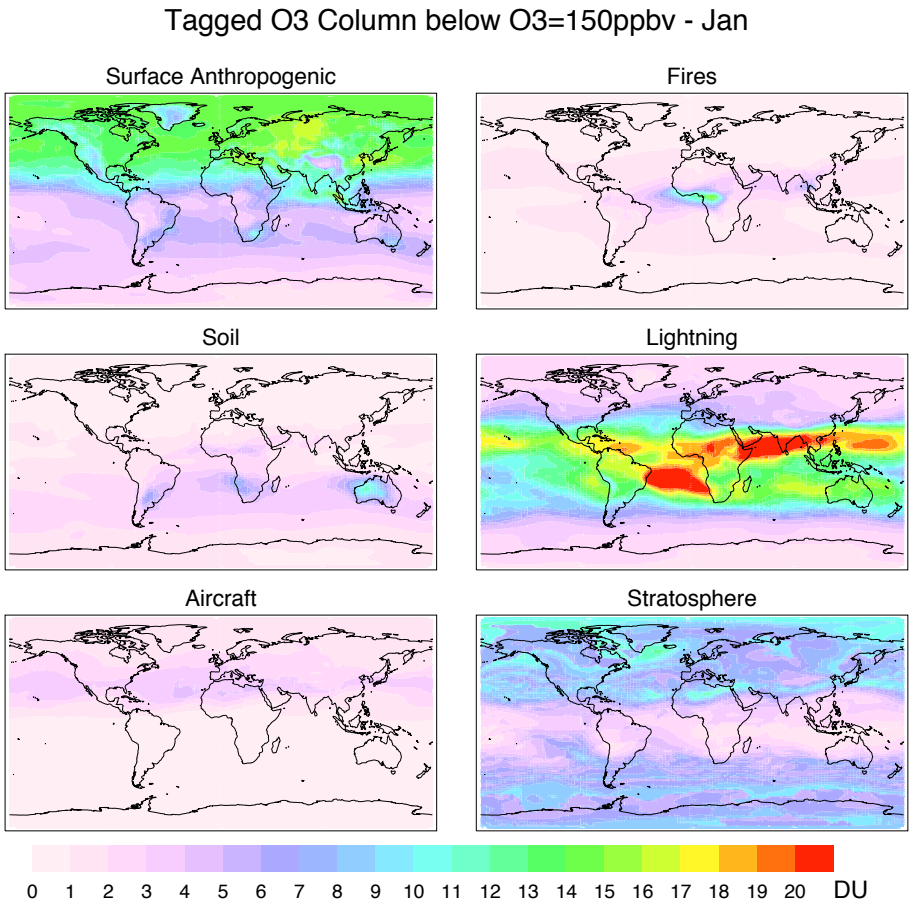

Fig. 1. Tropospheric columns of each tagged ozone source for January 2008. Stratospheric contribution is determined as the difference between total ozone and tagged ozone from all tropospheric sources. The chemical tropopause of O_3 at 150 ppbv is used.

GMDD
5, 1949–1985, 2012

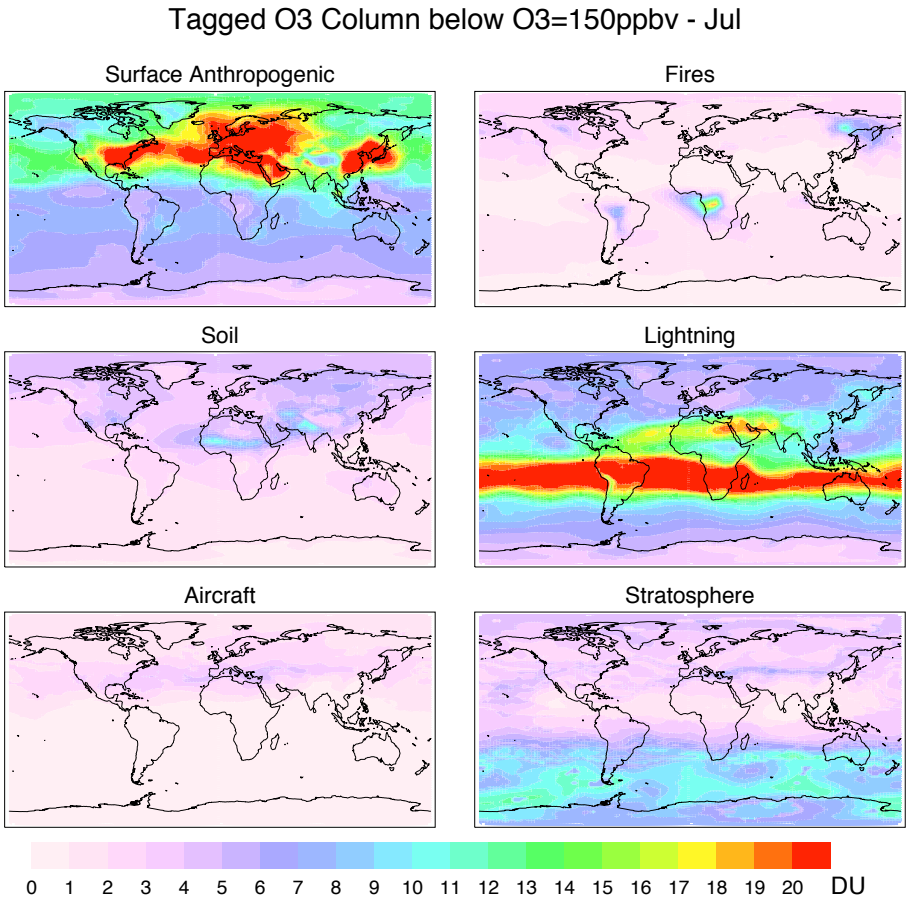

Fig. 2. As Fig. 1, for July 2008.

GMDD
5, 1949–1985, 2012

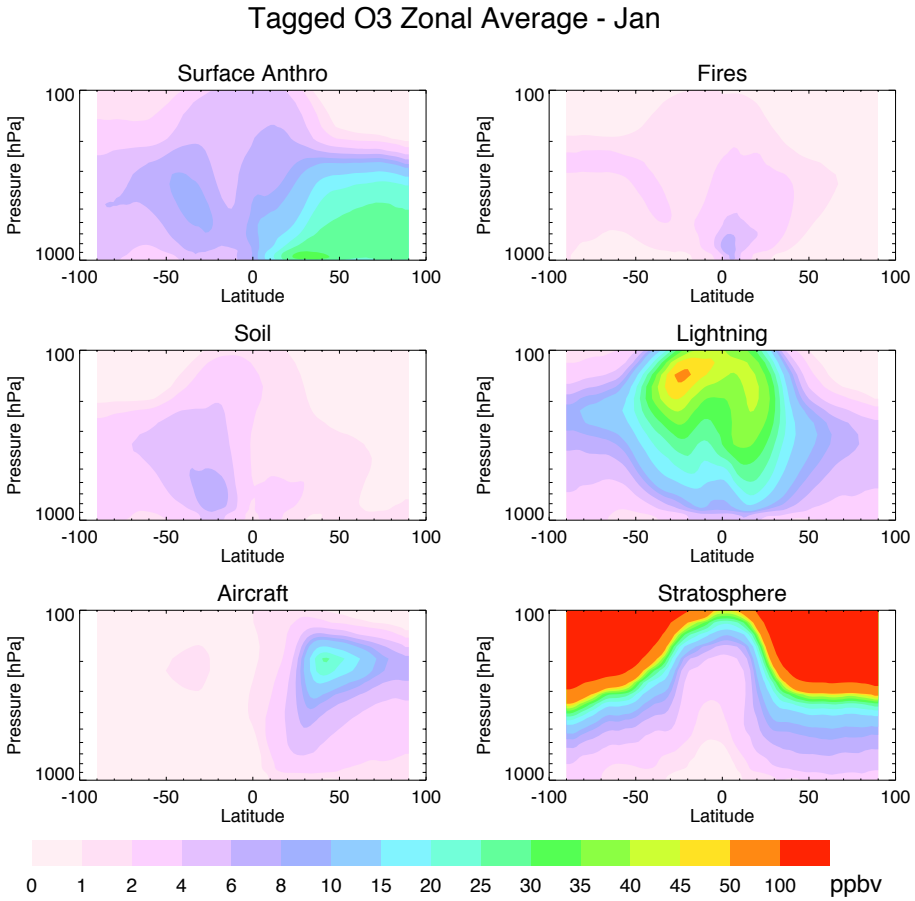

Fig. 3. Zonal average of each tagged ozone source for January 2008. Stratospheric contribution is determined as difference between total ozone and tagged ozone from all tropospheric sources.

GMDD
5, 1949–1985, 2012

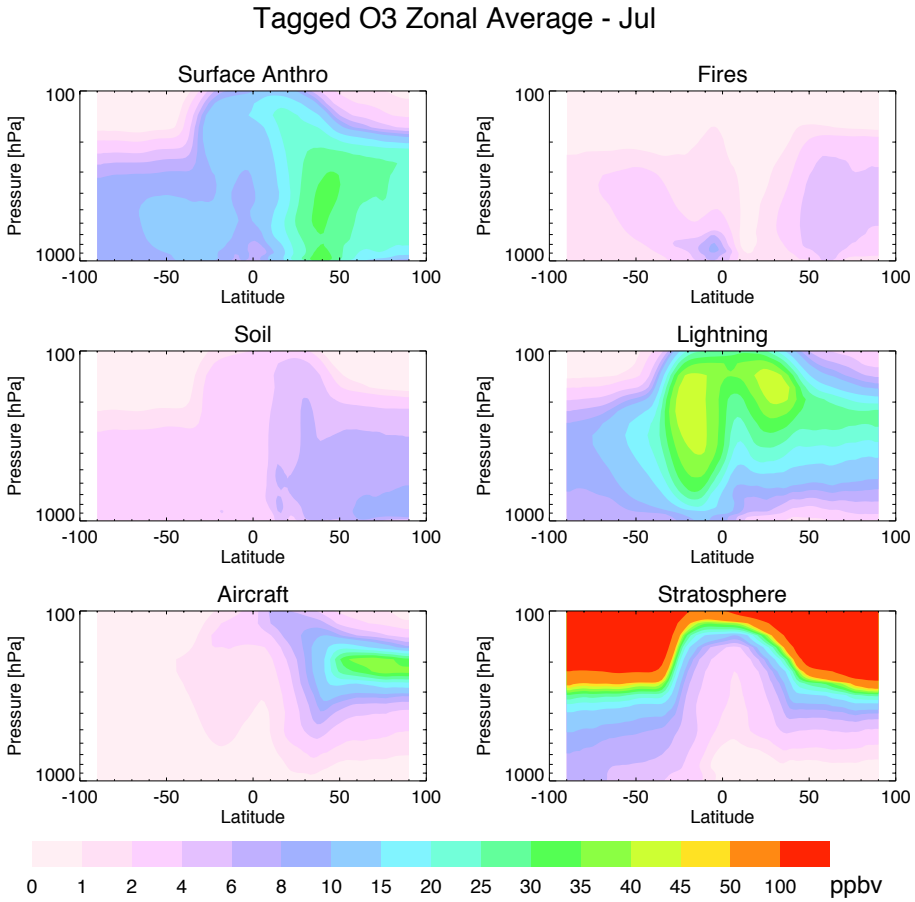

Fig. 4. As Fig. 3, for July 2008.

GMDD
5, 1949–1985, 2012

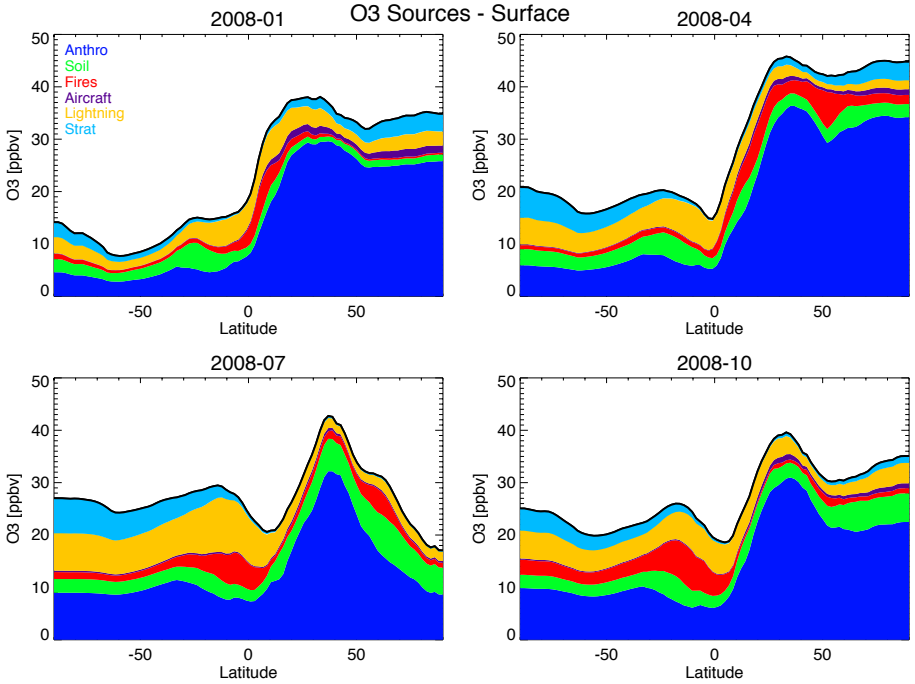

Fig. 5. Zonal average of tagged ozone source contributions at the surface, for January, April, July and October of 2008. Stratospheric contribution is determined as difference between total ozone and tagged ozone from all tropospheric sources combined.

GMDD
5, 1949–1985, 2012

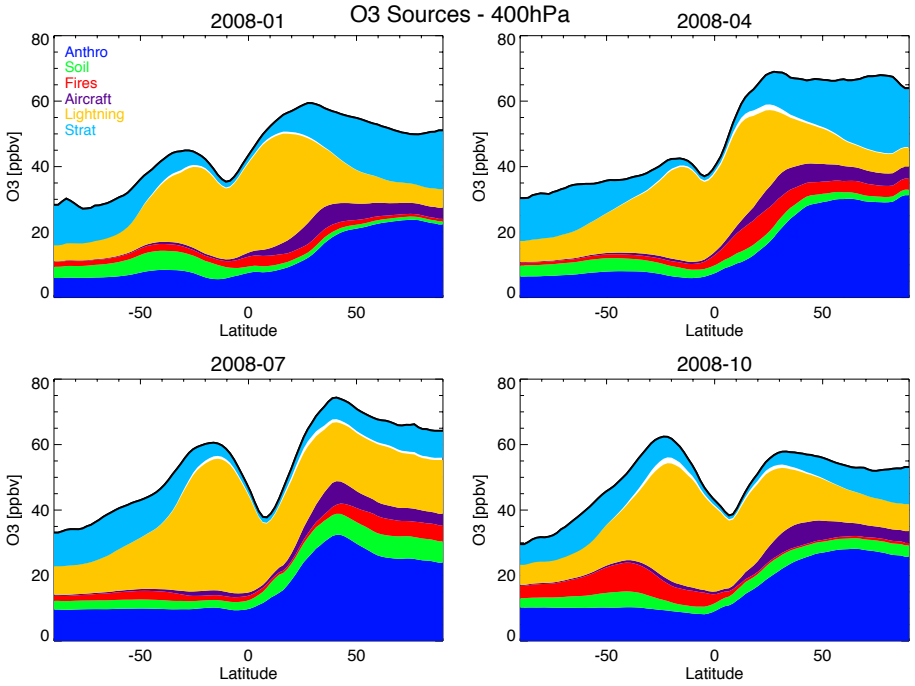

Fig. 6. As Fig. 5, for 400 hPa. The white region between the lightning and stratospheric contributions indicates the difference between tagging all sources and the sum of each tagged source.

GMDD
5, 1949–1985, 2012

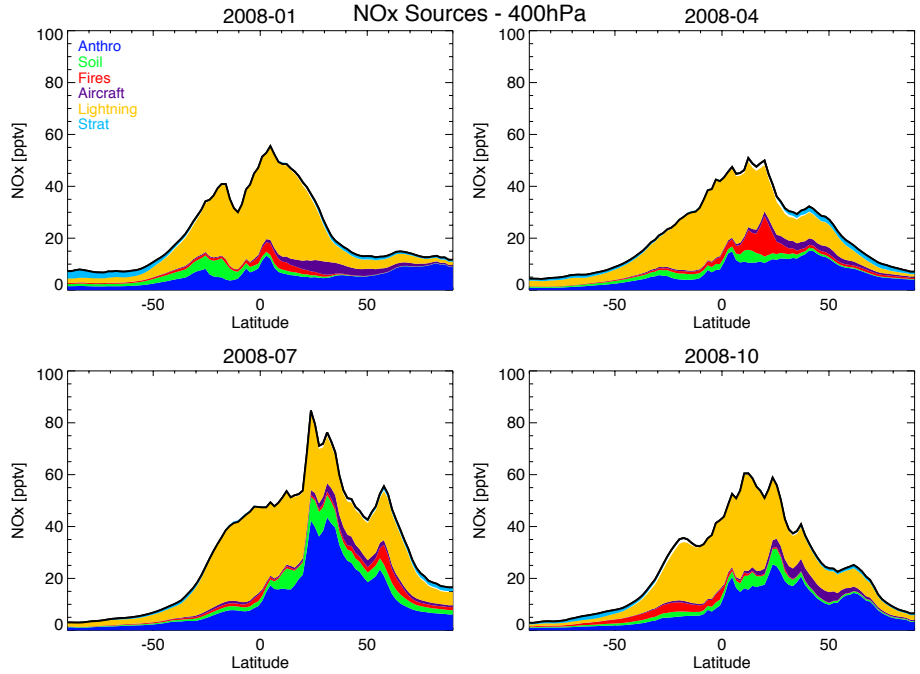

Fig. 7. As Fig. 5, for tagged NO_x source contributions at 400 hPa.

GMDD
5, 1949–1985, 2012

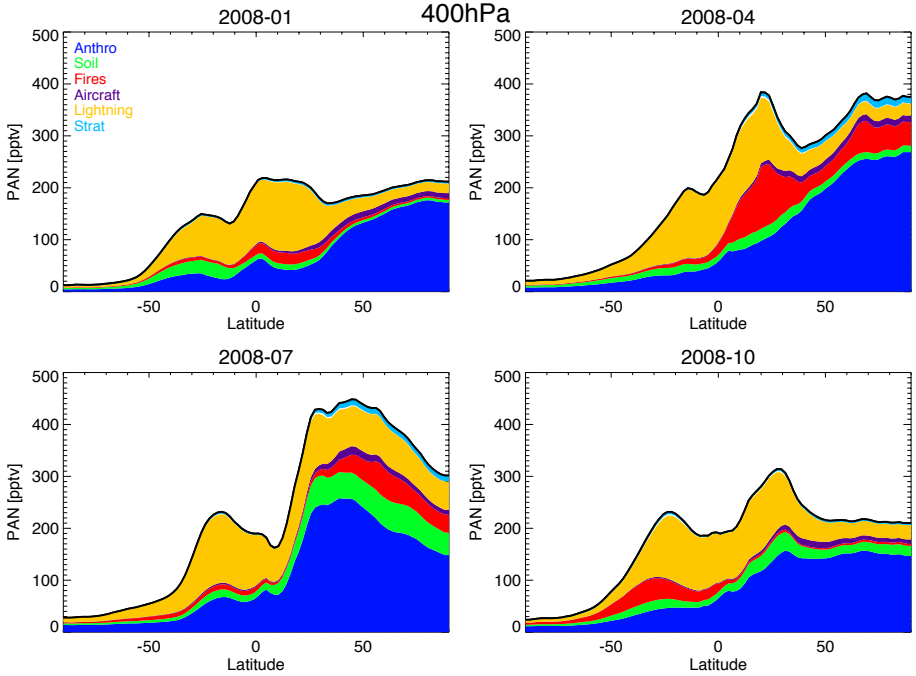

Fig. 8. As Fig. 5, for tagged PAN source contributions at 400 hPa.

GMDD
5, 1949–1985, 2012

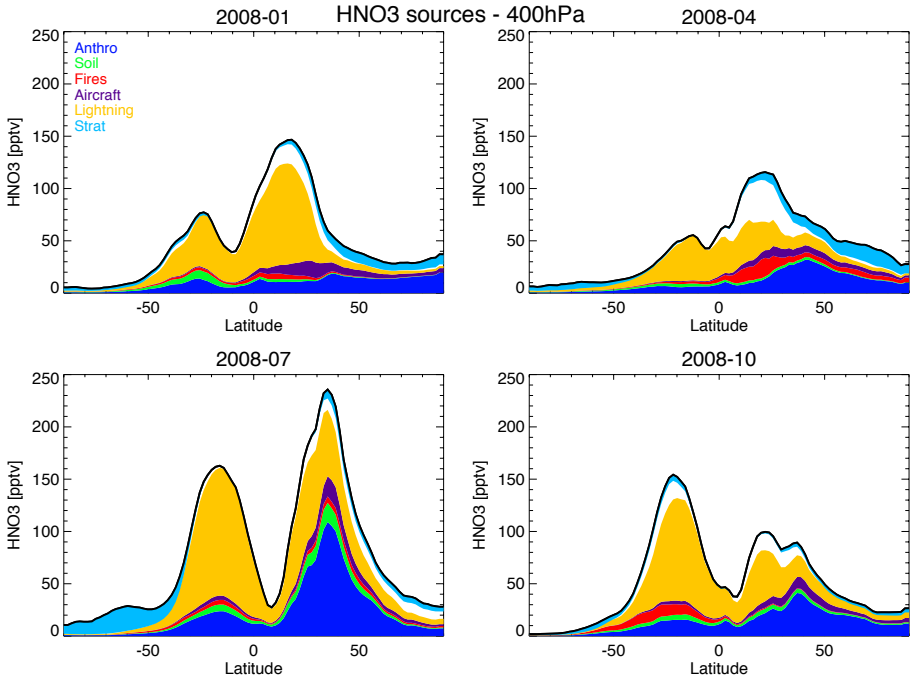

Fig. 9. As Fig. 5, for tagged HNO_3 source contributions at 400 hPa.

GMDD
5, 1949–1985, 2012

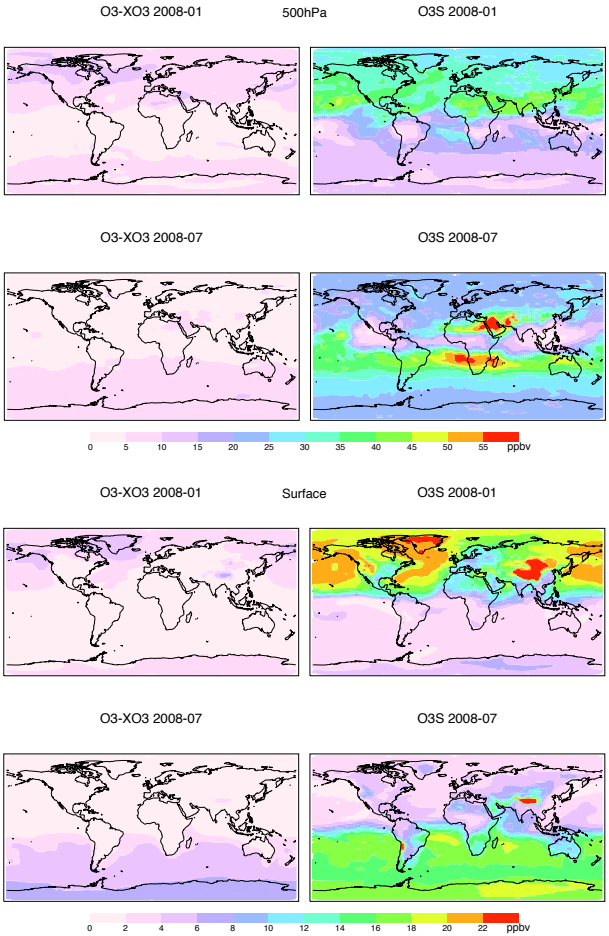

Fig. 10. Stratospheric ozone contribution from the tagged NO method (left) and from the stratospheric ozone tracer, O3S (right), at 500 hPa (top) and the surface (bottom).

GMDD
5, 1949–1985, 2012

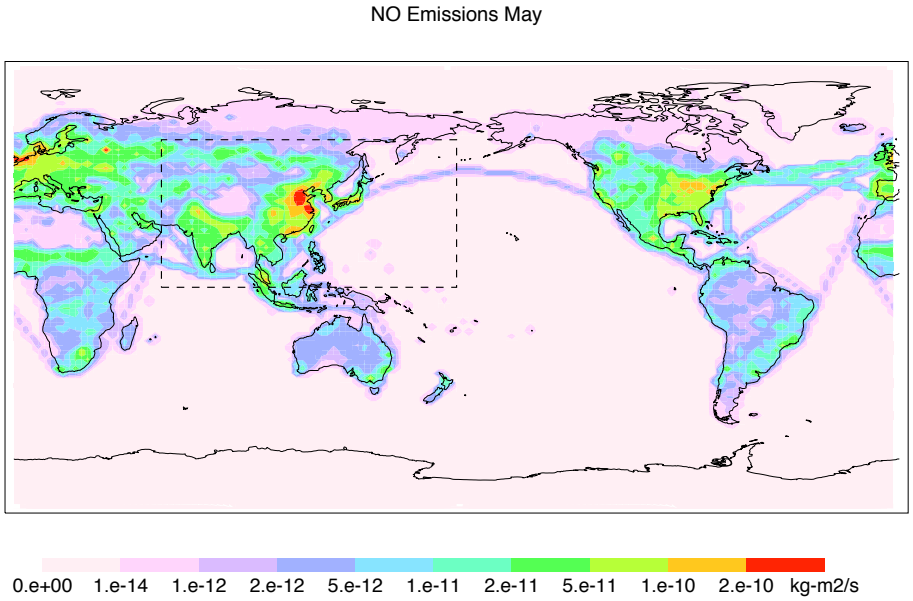

Fig. 11. NO surface emissions for May. Black dashed line shows region of tagged or perturbed emissions.

GMDD
5, 1949–1985, 2012

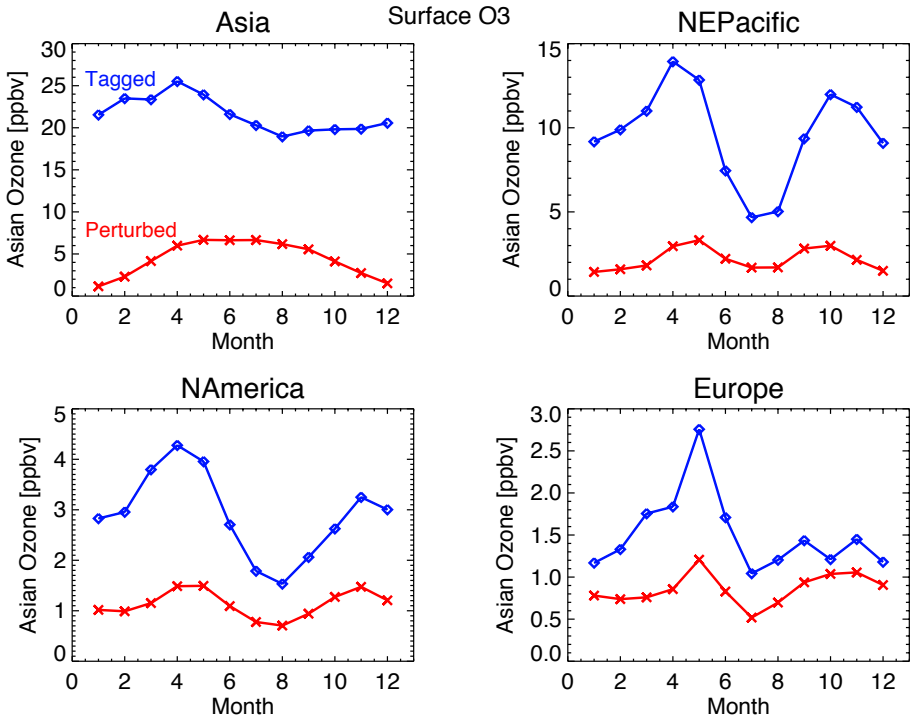

Fig. 12. Surface ozone attributed to Asian emissions based on tagged and perturbed NO_x emissions, averaged over four receptor regions, as a function of month. The perturbed contribution is 5 times the difference between the standard simulation and a simulation with 80 % NO_x emissions in Asia. The receptor regions are Asia (0°–60° N, 60°–180° E, same as emissions), NE Pacific (30°–55° N, 190°–235° E), N. America (15°–55° N, 235°–300° E) and Europe (30°–70° N, 0°–45° E).

GMDD
5, 1949–1985, 2012

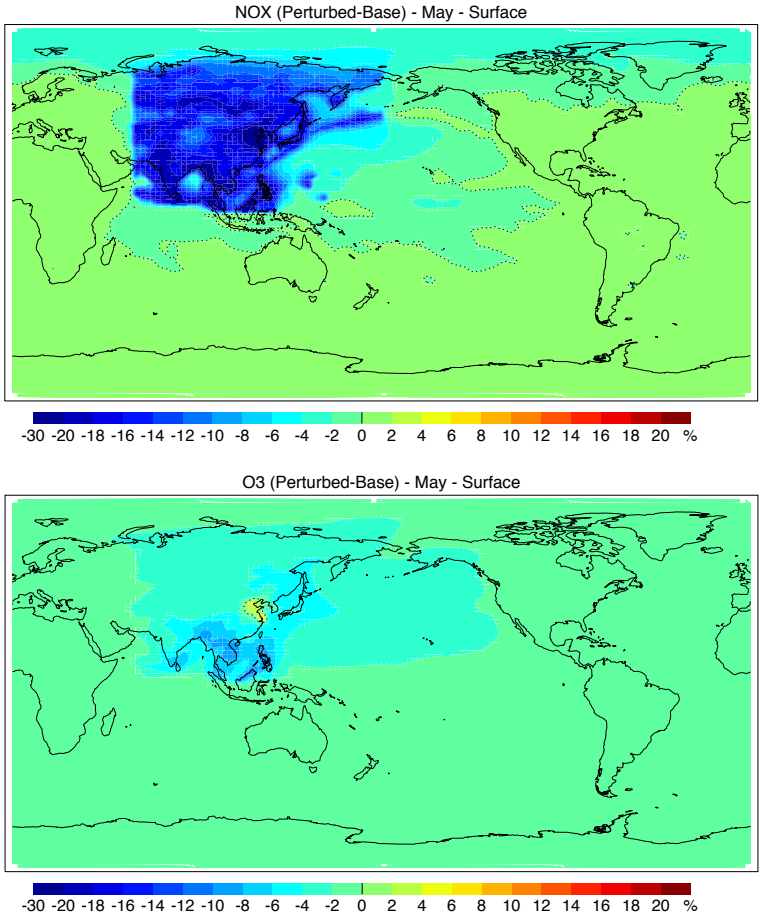

Fig. 13. Impact (%) on NO_x and O_3 in May due to reducing all NO sources in Asia by 20 %. Dotted line indicates the 0 % contour.

GMDD
5, 1949–1985, 2012

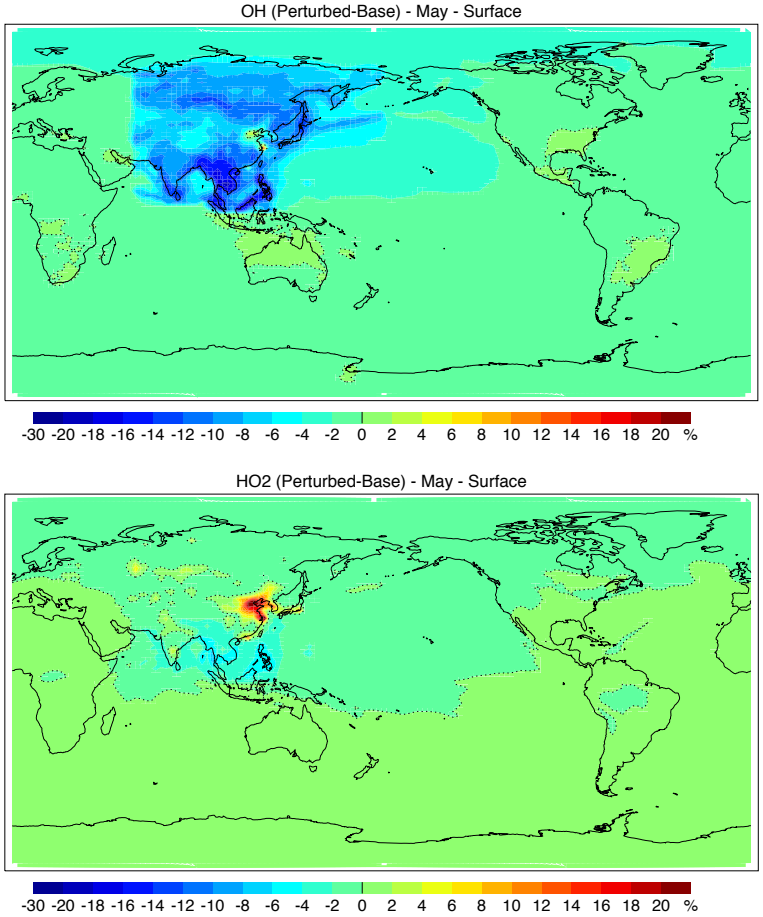

Fig. 14. As Fig. 13 for OH and HO_2.

GMDD
5, 1949–1985, 2012

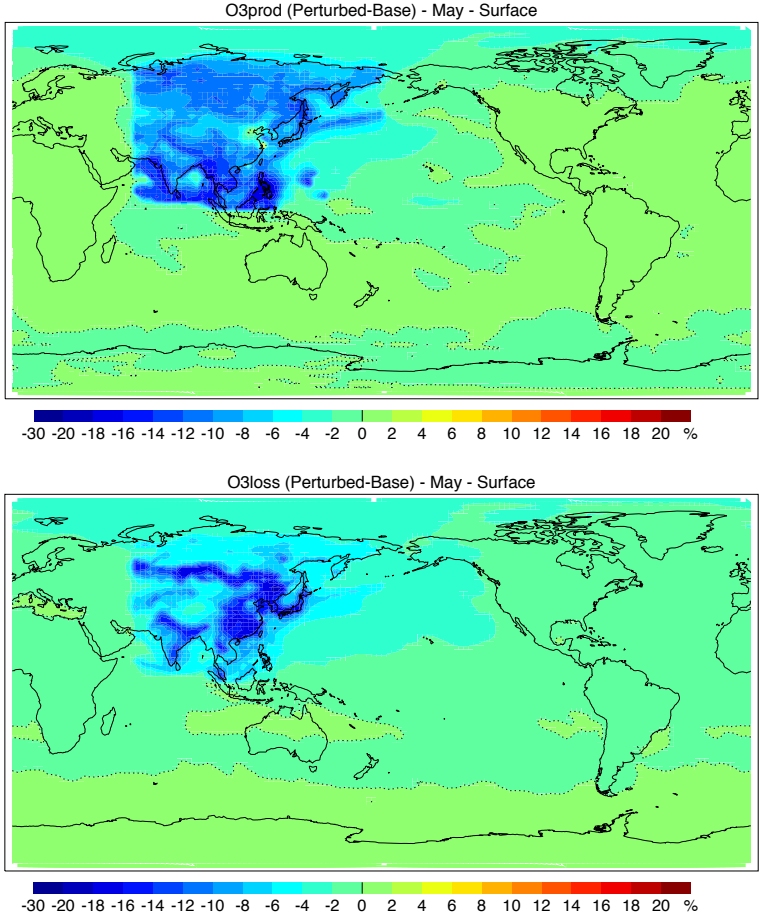

Fig. 15. As Fig. 13 for O_3 production and loss rates.

GMDD
5, 1949–1985, 2012